Cost Effective Deposition of Aluminium Oxide Layers

I.A. Khan[a,*], A. Rashid[a], A. Fatima[a], M.A.K. Shahid[a], T.H. Bokhari[b] and R. Ahmad[c]

[a]*Department of Physics, GC University, 38000, Faisalabad, Pakistan*

[b]*Department of Chemistry, GC University, 38000, Faisalabad, Pakistan*

[c]*Department of Physics, GC University, 54000, Lahore, Pakistan*

Abstract: Al_2O_3 surface-layers were deposited on Al substrates by thermal evaporation technique. Samples were treated for different (1 h, 2 h, 3 h, 4 h and 5 h) treatment time in open air environment by keeping the temperature (550°C) of the evaporator plate constant. XRD patterns revealed the emergence of Al_2O_3 H_2O (111), Al $(OH)_3$ (214) and Al_2O_3 (20 6) planes. Crystallinity of the above mentioned phases was attributed with treatment time. However, minimum treatment time to break oxygen hydrogen bonds and the formation of Al_2O_3 plane was 5 h. Crystallite size and compressive stress found in Al_2O_3 (2 0 6) plane were 14.31 nm 0.53 GPa respectively. SEM microstructure features revealed the formation of rounded grains, irregular patches and rods. AFM analysis exhibited the formation of dome shapes microstructures. The grain size and surface roughness were increased from 1 µm to 2.5 µm and from 35 nm to 115 nm respectively. This variation in surface roughness and grain sizes was associated with treatment time.

Keywords: Aluminium oxide, treatment time, XRD, growth, roughness.

1. INTRODUCTION

Materials in the form of surface layers have attention because of their remarkable surface properties which may differ significantly from their bulk characteristic making them more attractive for their industrial applications. Additionally, properties of surface layers could be changed by changing the deposition parameters. Recently, there has been growing interest to deposit surface layers of ceramic materials using different deposition techniques like chemical vapor deposition, physical vapor deposition, RF magnetron sputtering, DC glow discharges, plasma focus device and pulse laser deposition [1-7]. Among the promising ceramic materials, much more attention has been paid to form Al_2O_3 surface layers by virtue of their potential industrial applications such as defensive layers for metal reflectors in electronic and optical industries, temperature stabilization of satellites, dark mirrors and in semiconductors devices [8-11]. Moreover, growth of α-Al_2O_3 layer on Al substrate is of immense technological significance particularly for the electronic components by virtue of their outstanding dielectric properties [12]. Therefore, it was vital to deposit Al_2O_3 layers of desire surface properties using comparatively inexpensive techniques.

In this study, Al_2O_3 surface layers were deposited by simple and cost effective thermal evaporation technique in open air environment as function of treatment time. Throughout the experiment, the temperature (550°C) of the evaporated plate was constant. The deposited Al_2O_3 surface layers were characterized by x-rays diffraction (XRD), scanning electron microscopy (SEM) and atomic force microscopic (AFM) techniques in order to explored the surface properties like crystal structure, crystallite size, residual stresses, microstructure features, particle size and surface roughness of the deposited Al_2O_3 layers.

2. EXPERIMENTAL DETAILS

Al_2O_3 surface layers were deposited on Al substrates using thermal evaporation technique. The deposition processes was carried out in open air environment while the temperature (550°C) of evaporator plate remains constant. The temperature of the evaporator plate was recorded with digital temperature meter coupled with thermocouple. Keep in mind, temperature of the target material will be the same as that of evaporator plate since it was placed on the evaporator plate.

Al samples of diameter (1cm) and thickness (2 mm) were polished with silicon carbide abrasive papers of 2000 grit and ultrasonically cleaned in distilled water for 30 min. Al absorbed energy from the evaporator plate. The heated Al surface captured air species from the vicinity, reacted with each other results in the formation of Al $(OH)_3$, Al_2O_3 H_2O and Al_2O_3 phases. However, for 5 h treatment time, the only appearance of Al_2O_3 phase in the XRD results indicated that the deposited layer was free from hydrogen. Moreover, according to kinetic theory, the kinetic energy of the air species (like hydrogen and oxygen) increased with increasing treatment time since the species closed to the

*Address correspondence to this author at the Department of Physics, GC University, 38000, Faisalabad, Pakistan; E-mail: ejaz_phd@yahoo.com

ISSN: 1814-8085 / E-ISSN: 1927-5129/13 © 2013 Lifescience Global

evaporator plate absorbed heat resulted in the increase of their kinetic energy and it was found (XRD results) that 5 h treatment time was the minimum time at which hydrogen oxygen bonds was broken since only Al_2O_3 phase was present in the XRD results. Thus it was clear that the deposited layer was free from hydrogen. It was due to the fact that after bond breaking, hydrogen species left the active region due to smaller weight while oxygen species easily reacted with Al which could be due to high electronegativity differences results in the formation of Al_2O_3 layer.

3. RESULTS AND DISCUSSION

3.1. XRD Analysis

Figure **1** exhibited the XRD patterns of Al_2O_3 layers deposited in open air environment for different treatment time (1 h, 2 h, 3 h, 4 h and 5 h) keeping the temperature (550^oC) of the evaporator plate constant. For 1 h treatment time, XRD pattern revealed the emergence of two diffraction peaks appeared at 2θ values of 38.82^o and 45.2^o respectively which were correlated to Al_2O_3 H_2O (111) and Al $(OH)_3$ (214) phases [R. codes: 00-002-0291, 00-003-0146]. The crystallinity of Al_2O_3 H_2O (111) plane was higher than that of Al $(OH)_3$ (214) plane due to difference in their peak intensities. For 2 h treatment time, the crystallinity of the above mentioned phases abruptly changed in inverse fashion since their peaks intensities changed inversely. For 3 h treatment time, no abrupt change in the crystallinity was observed due to small variation in their peak intensities and broadening. For 4 h treatment time, again the crystallinity of the above mentioned phases abruptly changed in inverse fashion since their peaks intensities changed inversely. For 5 h treatment time, two new diffraction peaks appeared at 2θ values of 38.32^o and 44.67^o relating to Al and Al_2O_3 phases were observed. Actually, during the re-crystallization of previously formed phases and re-arrangement of the atoms forming solid solution resulted in the formation of aluminium oxide. The peak intensity of Al phase was smaller than Al_2O_3 phase thereby confirmed the better crystallinity of Al_2O_3 phase. This also confirmed that Al_2O_3 phase was more than Al phase in the deposited layer.

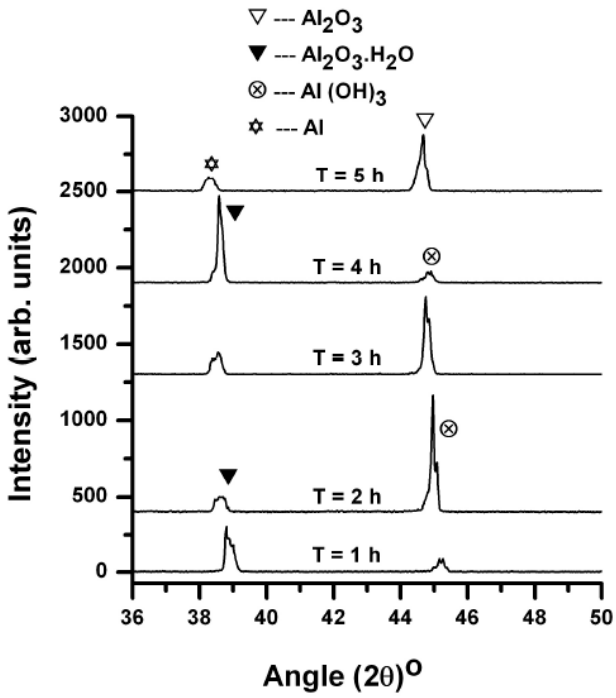

Figure 1: XRD patterns of Al_2O_3 layers deposited for different treatment times (1 h, 2 h, 3 h, 4 h and 5 h) at constant (550 ^oC) temperature.

XRD results demonstrated the formation of solid solution of Al and Al_2O_3 phases which could enhance the life time of the material. The more broadened diffraction peaks confirmed the formation of nano-crystallite since broadening was inversely proportional to crystallite size. However, broadening was associated with vacancies, point defects, lattice distortions and micro-strain developed during deposition process. Moreover, the concentrations of oxygen species associated with these parameters were directly coupled with the microhardness which increased the life time of the material. As the XRD patterns indicated the development of only Al and Al_2O_3 phases which confirmed the formation of pure Al_2O_3 layer. But still we could not say that the deposited layer was pure in nature because other environmental species may incorporated as impurities in amorphous phase since the present work was done in open air environment.

XRD data was employed to estimate the crystallite size of Al_2O_3 (206) plane observed for 5 h treatment time by using Scherer's formula [15].

$$Crystallite\ size = \frac{K\lambda}{FWHM\cos\theta}$$

where *K* was constant, λ was the wavelength of incident radiation, FWHM was the full width at half maxima and θ was the Bragg's angle. The estimated crystallite size of Al_2O_3 (206) plane was found to be 14.31 nm which confirmed the formation of nano-crystallite of aluminium oxide.

XRD data was also employed to estimate the residual stresses developed in Al_2O_3 layer. The up and

down shifting of diffraction peaks from their stress free values indicated the existence of residual stresses. The peak shifting from their stress free values was due to diffusion of oxides interstitially which distorted the lattice, creating point defects and vacancies. The peak shifting could also be due to the removal of hydrogen creating vacancies resulted in the development of defects. It is well known that more diffusion could take place at high temperature which may shift the diffraction peaks from their corresponding stress free values.

The strain $(\frac{\Delta d}{d})$ produced in Al_2O_3 (206) plane (observed for 5 h treatment time) was estimated by using the formula [16].

$$\frac{\Delta d}{d} = \frac{d(observed) - d(ICSD)}{d(ICSD)}$$

The estimated strain (- 1.55 × 10^{-3}) developed in Al_2O_3 (206) plane was multiplied with its young's modulus which gave the estimation of stresses. The young's modulus of Al_2O_3 layer ranged from 176 to 370 GPa depending on the deposition temperature and the purity of Al_2O_3 phase. The young's modulus of Al_2O_3 phase (500^{o}C temperature) was found to be 344 GPa. In our case, the deposition temperature was 550^{o}C which was very close to the above mentioned temperature for which the young's modulus of Al_2O_3 phase was 344 GPa. Thus, we multiplied the strain with 344 GPa (young's modulus) in order to estimate the residual stresses developed in Al_2O_3 phase at 500^{o}C temperature. The stress was found to be ~ - 0.53 GPa in Al_2O_3 layer deposited for 5 h treatment time where the negative sing indicated the compressive nature of stress.

3.2. SEM Analysis

Figure **2** demonstrated the SEM microstructure features of Al_2O_3 surface layers deposited for different treatment (1 h, 2 h, 3 h, 4 h and 5 h) time. All the samples were treated in open air environment for constant temperature (550^{o}C). For 1 h treatment time, the formation of rounded grains (ranged from 1 µm to 1.45 µm) showing irregular distribution was observed as shown in Figure **2A**. Some regions were featureless while the remaining regions showed colonies of rounded grains. Different grains of various dimensions and featureless surface appearance confirmed the formation of rough surface which was agreed well with the AFM results (discus later). Thus, grains of different dimensions, colonies, featureless microstructure appearance and total area covered by the colonies containing grains of various dimensions made the surface rough. For 2 h treatment time, again the formation of rounded grains and irregular patch of particles was observed (Figure **2B**). It was found that the size of rounded grains ranged from 1.3 µm to 2.5 µm while it ranged from 1.66 µm to 6.66 µm for irregular patches. The irregular patches which were bigger in size could be of Al $(OH)_3$ compound due to maximum peak intensity. The appearance of dark regions in the back ground of the particles also made the rough surface. For 3 h treatment time, the surface appearance was entirely changed, only irregular patches instead of rounded grains were observed. However, they were closely packed and separated through their grain boundaries (Figure **2C**). For 4 h treatment time, again an abrupt change in the microstructure appearance was observed. However, collection of rounded grains at one corner of the scanned micrographs was observed while the major portion of the scanned micrograph showed the formation of elongated horizontal rods (Figure **2D**). For 5 h treatment time, the surface morphology exhibited the formation of irregular patches distributing uniformly and covered the entire scanned portion. The uniform distribution of irregular patches covering the entire scanned area confirmed the compact nature of the layer. From the above discussion it was concluded that the formation of microstructure features like grain size, shape, their distribution and compactness were associated with the treatment time. Additionally, granular surface morphology was transformed into surfaces of irregular patches isolated by boundaries. It was well known that microhardness was attributed with the dimensions of particle sizes, smaller the particles more will be the microhardness [13]. In our case, the Al_2O_3 layer comprised of nano-particles confirmed the formation of hard layer which improved the strength, ductility and wear and corrosion resistance of the material. Additionally, during diffusion, lattice distortion and creation of vacancies and defects were responsible to increase the hardness of the deposited layer.

The basic mechanism behind the formation of Al_2O_3 layers was; Al placed on the evaporator plate absorbed energy, heated Al could react with air species results in the formation of nano-layers on Al surface. Keep in mind, Al could not evaporate at 550 ^{o}C in air environment since its melting point was 660.37 ^{o}C. Meanwhile, air species in the vicinity of target material increased their kinetic energy by getting heat from the evaporator plate.

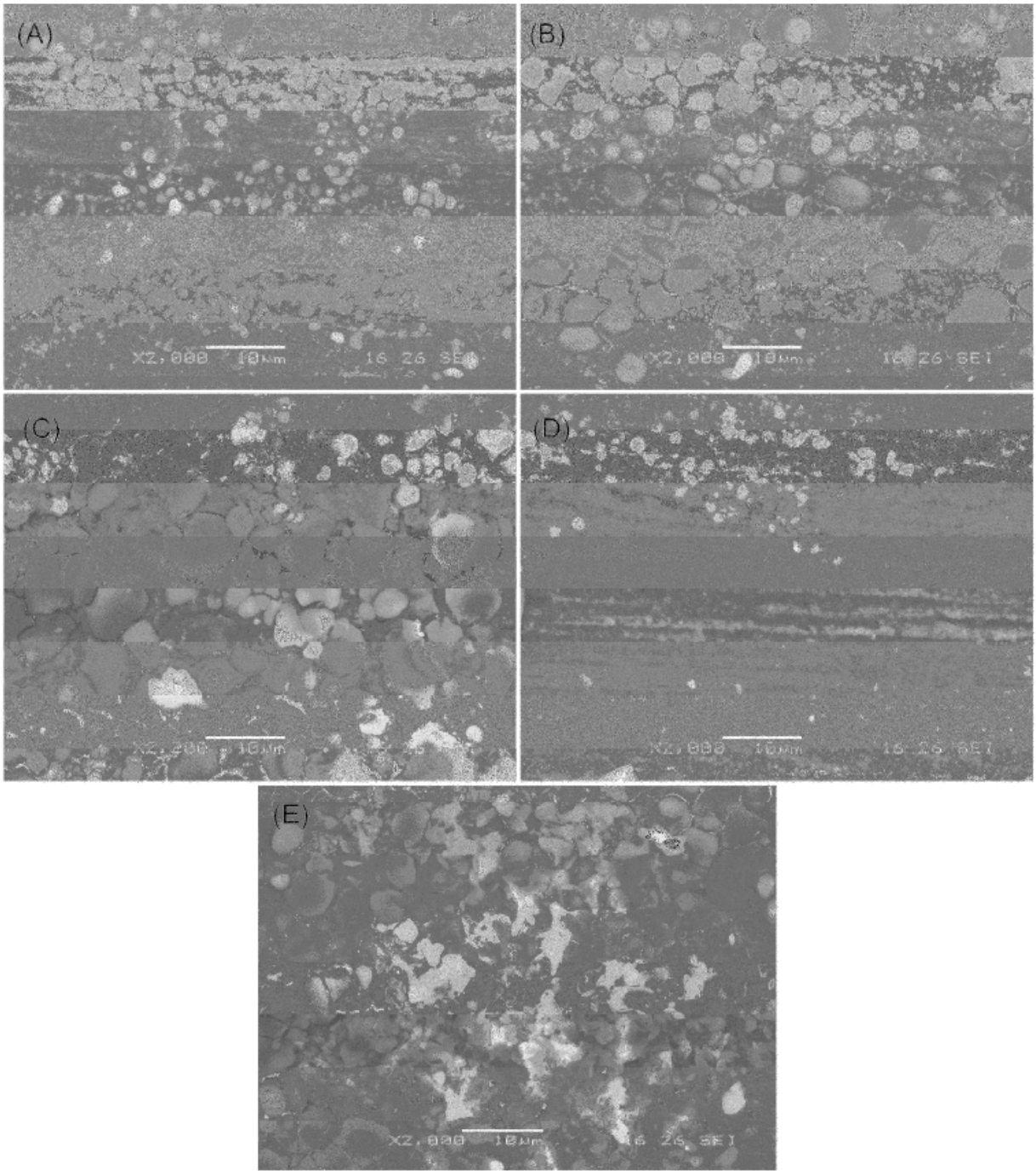

Figure 2: SEM microstructures of Al_2O_3 layers deposited for different (1 h, 2 h, 3 h, 4 h, and 5 h) treatment times.

However, these air species increased their kinetic energy with increasing treatment time. Thus up to 4 h treatment time, the kinetic energy of air species could not break the oxygen hydrogen bonds but collectively reacted with Al on target surface resulted in the formation of Al $(OH)_3$ and Al_2O_3-H_2O phases (XRD results). While for 5 h treatment time, the kinetic energy of air species was sufficient to break the oxygen hydrogen bonds, hydrogen species due to lighter weight removed from the active region whereas oxygen species reacted with Al due to sufficient energy resulted in the formation of Al_2O_3 layer which was free from hydrogen contents. That is why the breaking of hydrogen oxygen bonds and mobility of oxygen and hydrogen species were associated with increasing treatment time.

3.3. AFM Analysis

AFM analysis exhibited the surface morphology and roughness of aluminium oxide-hydrates and Al_2O_3

layers deposited for different (1 h, 2 h, 3 h, 4 h and 5 h) treatment time. AFM images revealed the formation of dome shape surface features. The different width and height of domes made the surface rough which was agreed well with the SEM results.

However, the dimensions (width and height) of domes depend on the treatment time whereas temperature and energy of the reactive species increased with increasing treatment time. Actually, the temperature and energy of the reactive species play a vital role to change the domes appearance and surface roughness. Figure **3E** exhibited the formation of domes of larger dimension which made rougher surface comparatively. Figure **4** showed the root mean square (rms) roughness of Al_2O_3 layers deposited for different

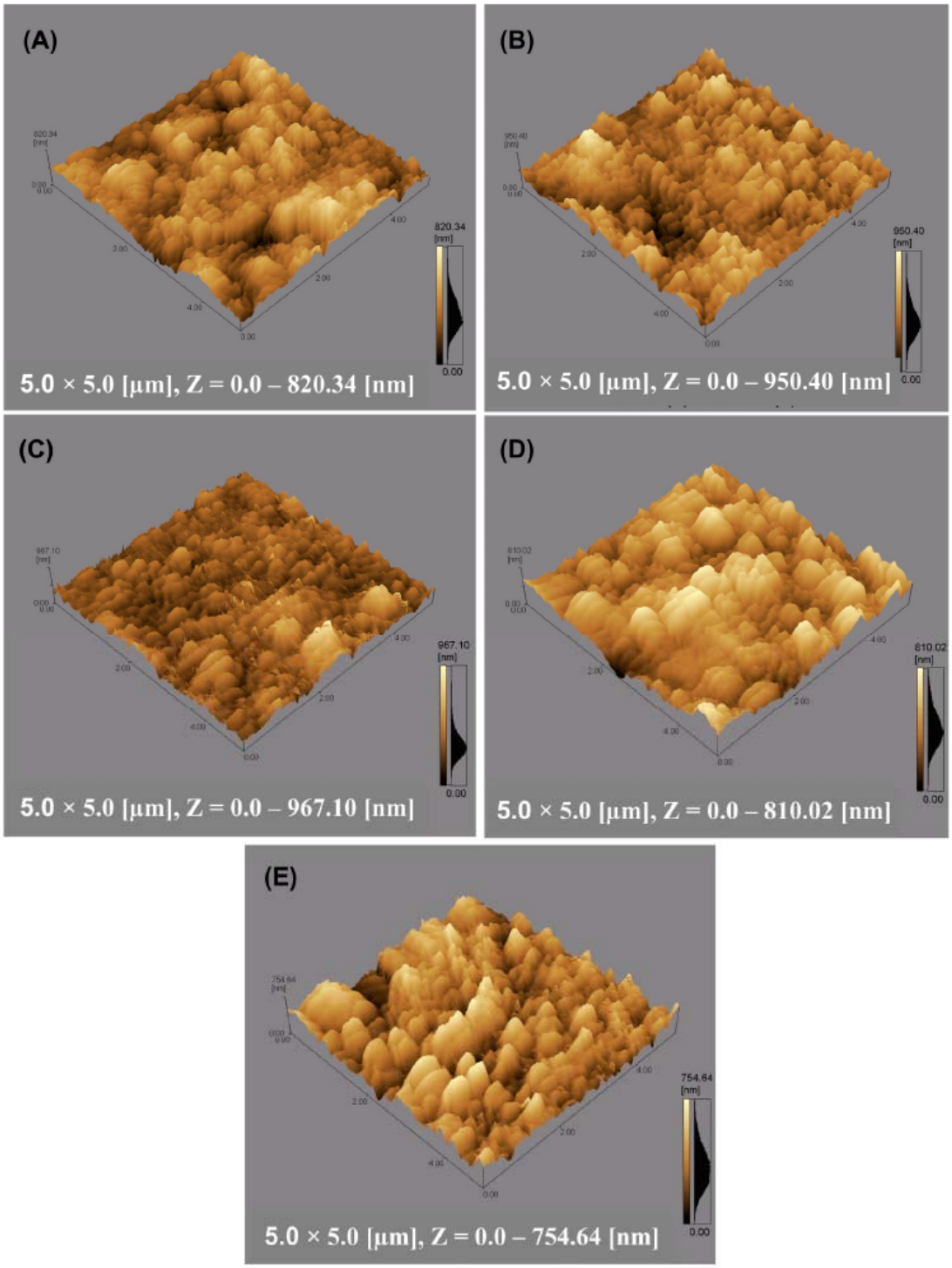

Figure 3: AFM images of Al_2O_3 surface layers deposited for different (1 h, 2 h, 3 h, 4 h, and 5 h) treatment times.

treatment time. Moreover, the roughness of the deposited layers increased (from 48 nm to 112 nm) with increasing treatment time. Thus the increase in surface roughness was attributed with increasing temperature which was associated with increasing treatment time. The increasing temperature actually increased the ad-atoms mobility which increased the growth rate of the deposited layers. This increase in ad-atom mobility changed the surface features which were responsible to change the surface layer properties.

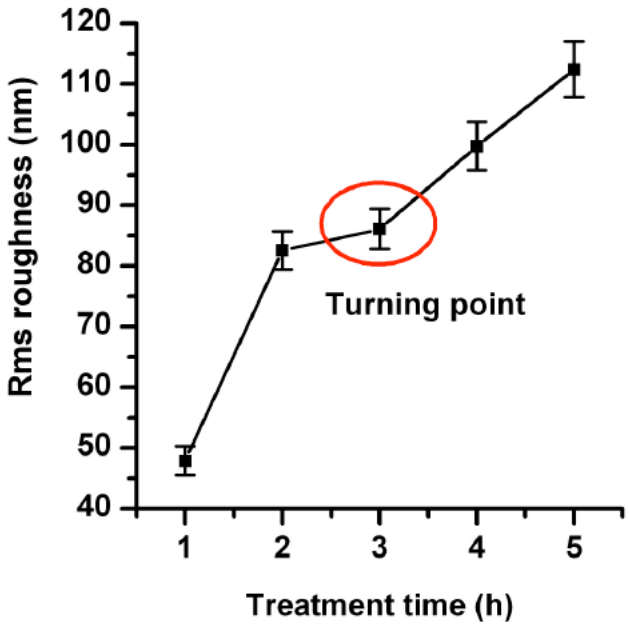

Figure 4: Variation of surface roughness as function of treatment time.

For careful investigation, the graph line was divided into three domains; (i) first domain (line joins the first two points) (ii) second domain (line joins the second and third point) and (iii) third domain (line joins the last three points). Sharp increase in rms values during first domain indicated the formation of porous layer which enhanced the diffusion of evaporated atoms results in rougher surface. Small increase in the rms values during second domain exhibited that the deposited layer was comparatively compact results in the decrease of surface roughness. During third domain, again a sharp increase in the surface roughness value was observed thereby indicated that again the layer became porous which was due to the interchange growth of different planes since the peak intensities varied with increasing treatment time. Moreover, for 3 h treatment time, a slightly decrease in surface roughness with increasing treatment time was observed. In order to understand this small decrease in surface roughness, more experiments were needed to explore the reason.

4. CONCLUSIONS

Al_2O_3 surface layers were deposited on Al by using thermal evaporator. Samples were treated for different (1 h, 2 h, 3 h, 4 h and 5 h) treatment time in open air environment for constant (550^{o}C) temperature. XRD patterns exhibited the formation of Al_2O_3 H_2O (111), Al $(OH)_3$ (214) and Al_2O_3 (20 6) phases. It was found that crystallinity of different planes varied with increasing treatment time. Five h treatment time was the minimum time at which oxygen and hydrogen species were more energetic having sufficient energy to break oxygen hydrogen bonds because the deposited layer was free from hydrogen species and only Al and O were present. Crystallite size and compressive stress observed in Al_2O_3 (2 0 6) plane were found to be 14.31 nm and 0.53 GPa respectively. SEM microstructure features demonstrated the formation of rounded grains (1 µm to 2.5 µm), irregular patches and rods. AFM images exhibited the formation of dome shape microstructures and their growth was associated with increasing treatment time. The grains of different dimensions (varied from 35 nm to 115 nm), formation of irregular patches and distribution of particles made the surface rough. Moreover, the changed in microstructure features like crystallinity, crystallite size, their distribution and the formation of irregular patches were correlated with the energy absorbed by the target material and the kinetic energy of the environmental species. Particularly, the kinetic energy of hydrogen and oxygen species was associated with increasing treatment time.

ACKNOWLEDGEMENTS

This work is fully supported by Director CASP, Prof. Dr. Riaz Ahmad, G C University Lahore for XRD, SEM and AFM analysis.

REFERENCES

[1] Cueff R, Baud G, Besse JP, Jacquet M. Study of thin alumina coatings sputtered on polyethylene terephthalate films. Thin Solid Films 1995; 266(2): 198-201. http://dx.doi.org/10.1016/0040-6090(96)80024-1

[2] Bodino F, Baud G, Benmalek M, Besse JP, Dunlop HM, Jacquet M. Alumina coating on polyethylene terephthalate. Thin Solid Films 1994; 241(1-2): 21-24. http://dx.doi.org/10.1016/0040-6090(94)90388-3

[3] Kim Y-C, Park H-Ho, Chun JS, Lee W-J. Compositional and structural analysis of aluminum oxide films prepared by plasma-enhanced chemical vapor deposition. Thin Solid Films 1994; 237(1-2): 57-65. http://dx.doi.org/10.1016/0040-6090(94)90238-0

[4] Astrand M, Selinder TI, Fietzke F, Klostermann H. PVD-Al_2O_3-coated cemented carbide cutting tools. Surf Coat Technol 2004; 188-189: 186-92. http://dx.doi.org/10.1016/j.surfcoat.2004.08.021

[5] Yang C-S, Kim J-S, Choi J-W, Kwon M-H, Kim Y-J, Choi J-G, *et al*. XPS study of aluminium oxides deposited on PET thin film. J Ind Engineering Chemistry 2000; 6 (3): 149-156.

[6] Khan IA, Hassan M, Ahmad R, Qayyum A, Murtaza G, Zakaullah M, *et al*. Nitridation of zirconium using energetic ions from plasma focus device. Thin Solid Films 2008; 516: 8255-63. http://dx.doi.org/10.1016/j.tsf.2008.03.012

[7] Villarreal-Barajas JE, Escobar-Alarcón L, Camps E, González PR, Villagrán E, Barboza-Flores M. Thermoluminescence response of aluminium oxide thin films to beta-particle and UV radiation. Superficies y Vacío 2001; 13: 126-29.

[8] Gan L, Gomez RD, Castillo A, Chen PJ, Powell CJ, Egelhoff Jr WF. Ultra-thin aluminium oxide as a thermal oxidation barrier on metal films. Thin Solid Films 2004; 415: 219-23. http://dx.doi.org/10.1016/S0040-6090(02)00622-3

[9] Stojadinovic S, Vasilic R, Nedic Z, Kasalica B, Belca I, Zekovic LJ. Photoluminescent properties of barrier anodic oxide films on aluminum. Thin Solid Films 2011; 519(11): 3516-21. http://dx.doi.org/10.1016/j.tsf.2011.01.188

[10] Deshpandey C, Holland L. Preparation and properties of Al_2O_3 films by D.C. and R.F. magnetron sputtering. Thin Solid Films 1982; 96(3): 265-70. http://dx.doi.org/10.1016/0040-6090(82)90251-6

[11] Roth Th, Kloos KH, Broszeit E. Structure, internal stresses, adhesion and wear resistance of sputtered alumina coatings. Thin Solid Films 1987; 153(1-3): 123-33. http://dx.doi.org/10.1016/0040-6090(87)90176-3

[12] Alwitt RS. The Anodic Oxidation of aluminum in the presence of a hydrated oxide. J Electrochem Soc 1967; 114: 843-48. http://dx.doi.org/10.1149/1.2426751

[13] Nie X, Leyland A, Song HW, Yerokhin AL, Dowey SJ, Matthews A. Thickness effects on the mechanical properties of micro-arc discharge oxide coatings on aluminium alloys. Surf Coat Tech 1999; 119: 1055-60. http://dx.doi.org/10.1016/S0257-8972(99)00089-4

[14] Nie X, Meletis EI, Jiang JC, Leyland A, Yerokhin AL, Matthews A. Abrasive wear/corrosion properties and TEM analysis of Al_2O_3 coatings fabricated using plasma electrolysis. Surf Coat Tech 2002; 149: 245-51. http://dx.doi.org/10.1016/S0257-8972(01)01453-0

[15] Cullity BD, Stock SR. Elements of X-ray Diffraction, 3rd ed. Prentice Hall, New-Jersey 2001.

[16] Rawat RS, Arun P, Vedeshwar AG, Lee P, Lee S. Effect of energetic ion irradiation on CdI2 films. J Appl Phys 2004; 95/12: 7725-30. http://dx.doi.org/10.1063/1.1738538

Received on 12-02-2013 Accepted on 29-03-2013 Published on 04-04-2013

http://dx.doi.org/10.6000/1927-5129.2013.09.33

© 2013 Khan *et al*.; Licensee Lifescience Global.
This is an open access article licensed under the terms of the Creative Commons Attribution Non-Commercial License (http://creativecommons.org/licenses/by-nc/3.0/) which permits unrestricted, non-commercial use, distribution and reproduction in any medium, provided the work is properly cited.